

Correlation Analysis Between International Roughness Index (IRI) and Pavement Distress by Neural Network

By

Jyh-Dong Lin
Professor
jyhdongl@cc.ncu.edu.tw

Jyh-Tyng Yau
Graduate Student
s8322019@cc.ncu.edu.tw

Liang-Hao Hsiao
Graduate Student
Lhhsiao@cyit.edu.tw

Department of Civil Engineering
National Central University, Taiwan
Taoyuan, Chungli, 32054, Taiwan
Tel: 886-3-4581080
Fax: 886-3-4227183

Paper Submitted for Presentation and Publication at the
82th Annual Meeting in January 2003 of the
Transportation Research Board, Washington, D.C.

ABSTRACT

In 1999, the Taiwan Highway Bureau imported ARAN (Automatic Road Analyzer), a specially equipped car that provides speedy and accurate pavement inspection, and outputs the measured pavement roughness as IRI (International Roughness Index). Since then, the traditional road-inspector visual inspection performed at network level pavement inspection had the tendency to be replaced by automatic inspection devices. Engineers also have gradually started to pay attention to IRI index. However, some pavement distress deterioration conditions are unique to Taiwan due to the island climate and special characteristics of the traffic and axle load. In this paper, analysis of the relationship between IRI and pavement distresses is performed based on a back-propagation neural network methodology to evaluate the applicability of IRI to be treated as a critical representation index of pavement performance. Moreover, the effects of distinct distress types and their extent on IRI can also be analyzed to infer roadwork benefit.

Based on a back-propagation neural network we construct in this research, IRI may be predicted accurately from distress rating results obtained from pavement video images, which is recorded by a camera mounted on ARAN. The correlation coefficient between IRI and the distress variables reaches 0.944, which shows that IRI may completely reflect pavement distress conditions. Thus, it is feasible to use IRI as a pavement performance index. Using IRI may simplify inspection works. Obviously, different distress types differently impact IRI. We find the definite effect of each distress type on IRI by sensitivity analysis. Thus, we may infer the improvement in the IRI resulted from certain extent or amount of repair for each distress. However, even if local road authorities are not equipped with automatic inspection devices, an accurate IRI is still obtainable via the present visual inspection method based on the back-propagation neural network we propose. Then, based on this IRI further optimization analysis can proceed. [1]

Key Words: distress, international roughness index, back-propagation neural network, visual inspection

INTRODUCTION

Pavement roughness is a characteristic which may be measured by various automatic multifunctional pavement measuring devices, and which may be expressed using the International Roughness Index (IRI), an international parameter used to measure pavement roughness conditions. It differs from RN, PSR and other common roughness indexes that depend on subjective human experts' evaluations. Besides, IRI is more convenient than any other index created by visual evaluation processes, such as PCI, etc.[2] This research examines the efficacy of the IRI pavement condition index to confirm that it not only conforms to the international trends, but avoids effects of unreliable and inconsistent results by personal factors in determining index value.

Pavement surface roughness is a major concern associated with driving quality. [3] Since pavement roughness causes an increase in vertical stress received by pavement and the aggravation of pavement fatigue, pavement roughness certainly accelerates pavement distress deterioration. Furthermore, pavement roughness indicates pavement surface deformation, which may affect pavement drainage, drive safety, etcetera. [4] Any pavement distresses will also result in a deterioration of the pavement roughness index value. Thus, the above shows that pavement distress and pavement roughness have a mutually causal relationship, affecting one another in both directions.

Although both IRI and specific distress types should be considered in determining road work activities, and performing more "near project level" analysis cannot only rely on the IRI data collection, data collection tasks of enormous road networks consume substantial cost of money and time. If we can reinforce the concepts that IRI may completely reflect pavement distress conditions and that there is a relationship between IRI and certain pavement distresses, IRI data will become more valuable information for ministry of transportation to analyze and evaluate the overall network situation. Moreover, it becomes more reasonable to only rely on the IRI to determine which road section among network may needs maintenance or improvement when it is difficult to collect distress measurement and imaging under limited resources conditions.

BACKGROUND

Pavement Deterioration

A pavement maintenance system should have the ability to perform present pavement performance evaluation and future performance prediction. [5] Pavement performance is determined by both distress degree and distress extent. To obtain a long-term pavement deterioration prediction model, a detection model of pavement deterioration starting from when it first provides service to the time it begins deterioration, as well as the annual deterioration condition during deterioration, should be established. Most time-based prediction models depend on annual structure numbers, annual equivalent standard axles, deflection resilient modulus, pavement thickness, crack level before repair, and climatic factors. After establishment of a deterioration model of each distress type, the effects of the each crack type to IRI are created, and then the deterioration model of IRI is as follows: [6]

$$\Delta\text{IRI} = K_{gp}[\Delta\text{IRI}_s + \Delta\text{IRI}_c + \Delta\text{IRI}_r + \Delta\text{IRI}_l] + \Delta\text{IRI}_e$$

ΔIRI : total incremental change in IRI during the analysis year

ΔIRI_e : incremental change in IRI due to environment during the analysis year

ΔIRI_s : incremental change in IRI due to structure deterioration during the analysis year

ΔIRI_c : incremental change in IRI due to cracking during the analysis year

ΔIRI_r : incremental change in IRI due to rutting during the analysis year

ΔIRI_l : incremental change in IRI due to potholing during the analysis year

K_{gp} : calibration factor

While a deterioration prediction model of IRI may be constructed based on long-term data measured from actual road sections (not our main topic), the modeling procedures described above are not necessarily applied. If the correlation between each type of distress and roughness, and the proof that IRI may completely reflect pavement deterioration, may be obtained, then it is simple and reasonable to regard IRI as pavement performance index without considering other distress types, and to represent the change of performance of the pavement life cycle as the change of IRI. Moreover, deterioration models of other distress types combining two or more distress types that occur simultaneously may also be created by using the constructed

deterioration model of IRI.

Types of Distress

The main objective of pavement management research is to achieve complete systematization and automation of pavement management and detection. However, even in a developed country, part of the measurement of pavement conditions still depends on manual visual inspection, whose data should be integrated and validated with data obtained from multi-functional measuring devices.

To understand the correlation between pavement roughness and all kinds of distress, analysis and prediction based on a neural network are performed to examine the correlation of pavement roughness and ten types of distresses that commonly found in Taiwan, listed as follows:

1. Rutting
2. Alligator cracking
3. Cracking
4. Digging /patching (digging for the purpose of installing pipes, wires, etc. and subsequent patching)
5. Potholes
6. Corrugation
7. Man-holes
8. Stripping
9. Patching
10. Bleeding

PAVEMENT INSPECTION

125 road sections with a length of 1 km are used in the collection of data, including provincial highways and county roads. All pavement information collection is performed by ARAN (Automatic Road Analyzer), an automatic road analyzer recommended by The World Bank and Federal Highway Administration (FHWA). First, we use ARAN system to automatically obtain the roughness index value and rutting depth of each road section by using a laser roughness measuring device and supersonic rutting measuring device which are mounted on ARAN. The examination and data recording of ten pavement distress types are done manually in the laboratory by determining the distress type and counting its corresponding distress amount or

extent based on the pavement image obtained from the image retrieval system, which is one of ARAN's subsystems. Roughness data, rutting data, and distress data are integrated and outputted by the software package, VIEW 4.55.

Generally, pavement condition produces a normal distribution. For example, a road section with an IRI of over 6, indicating heavy deterioration, has a lower frequency. Similarly, a road section with IRI under 2 also has a lower frequency. Data of normal distribution is usually unsuited to neural network analysis. If the road measurement is performed using random samplings, only a few of the extremely worst or best road sections may be obtained. And thus the results of IRI are difficult to analyze and use for predictions. As a result, the apparent ratio of the best and worst road sections of the 125 samples is much higher than its actual frequency. For the purpose of training the neural network, the data set of 125 records is divided into 2 sets: 100 records as the training data set and the other 25 records as the testing data set.

Roughness Measurement

The roughness measurement is performed by the Roughness Subsystem of ARAN, which consists of a roughness computer, laser SDP software, the accelerometer (only one is needed), and the roughness lasers (the laser subsystem is similar to the Laser South Dakota Profile (SDP)). This subsystem is an inertia measurement device. The sensitivity factor has to be considered in the roughness measurement. The sensitivity factor in this research is set to 0.6 m: that is, a longitudinal profile less than 0.6 m may be eliminated. This sensitivity factor is suitable for the general speed of a motor vehicle. It is recommended that the length of a single measured road section is not more than 73 km (45 miles). Additionally, for wavelengths filtration, we consider only the wavelength less than 91 m to avoid erroneous determinations caused by non-roughness factors. In this research, the roughness measurement output is represented as an IRI value.

Rut Depth Calculation

The rut depth calculation is performed by the Smart Bar subsystem of ARAN, which consists of a smart bar computer and ultrasonic software, an ultrasonic controller, retractable ultrasonic extension wings, ultrasonic sensors, and ultrasonic driver boards. The smart bar computer measures the time between the transmission

and the reception of signals for each ultrasonic sensor. Then, it calculates the distance to the road based on the speed of the sound and the rut depths for the wheel paths. For data collection, 19 ultrasonic sensors are mounted to instrument enclosures, each separated by a distance of 10cm. When needed, extension wings are used to add length to the smart bar. The right and left extensions combined provide a full lane width measurement of 3.7 m. Sensors are accurate to 1 mm.

Pavement Condition Rating

A high quality video camera is mounted to the underside of the vehicle's ceiling and is aimed through ARAN's front windshield to record the picture. The pictures are recorded by using a video cassette recorder (VCR). The image data details road conditions, giving the engineer a secondary visual inspection of the problem surface after the condition rating has been completed. The camera takes 30 pictures per second, supplying a resolution image. The pavement image contains data such as the road section name, the direction, the number of lane, the mileage, the speed, etc. After the outdoor picture collection is finished, files are processed by the software package VIEW 4.55. Then, the videotape is displayed on video monitors. The operator running the rater keyboard bases his judgements on distress types and surface areas shown on the videotape output display. Rating results, rutting and IRI values are integrated by VIEW 4.55.

Data Processing

Within a 1-km-road section, for alligator cracking, cracking, digging/patching, corrugation, patching, bleeding, and stripping inspections, we observe what proportion of the road section contains these distress types by visual ratings based on the pavement videotape images. We consider 20m as one measurement unit because, in general, the unit of partial road works in Taiwan is 20m. For instance, if a 200-m digging/patching occurs on a road section with the length of 1 km, then its patching value is 10. Potholes are divided into severe potholes and mild potholes, and the number of their occurrences within a 1 km segment is recorded. The man-hole is categorized into a severe or mild man-hole and the variable recorded is simply the number of them. Furthermore, since the 125 samples of data contain provincial highways and county roads, one additional attribute, road level, is added into the analysis to classify provincial highways and county roads into categories 1 and 2

respectively.

We only consider the surface area of alligator cracking, cracking, digging/patching, corrugation, patching, bleeding, and stripping without taking the degree into consideration in our neural network analysis since the distress extent or amount is measurable, while distress degree is uncertain and easily effected by subjective opinions of investigators using visual ratings based on the pavement videotape images. However, distress surface areas and distress degree are in fact related. In the future, if consistency of investigator's judgements upon the distress degree can be ensured, it will be considered as one of the measurement variables, and thus the correlation coefficient of the model can be increased.

NEURAL NETWORK CONSTRUCTION

Neural Networks have been widely used in other areas of pavement analysis. [7,8] A back-propagation neural network is applied in this research. Parameters of network design are shown in table 1. The Input layer has 14 nodes (variables): The road level, left rutting, right rutting, alligator cracking, cracking, digging/patching, mild potholes, severe potholes, patching, bleeding, corrugation, stripping, mild man-holes and severe man-holes are inputted in the above order, as shown in table 2. There are 6 nodes at the hidden layer, which is set based on generally accepted knowledge in this field. Within a reasonable range, the number of nodes at a hidden layer, about half of the total number of nodes at the input and output layers, has only slight effects on the training process of the neural network. The output layer has only one node (variable), the roughness index. Artificial neural connections of size of 90 ($14 \times 6 + 6 \times 1$) are constructed using 14 nodes at the input layer, 6 nodes at the hidden layer, and 1 node at the output layer, illustrated in figure 1. All included variables are normalized. Computation between two nodes of different layers in the neural network is provided by four transfer functions as shown below. The most appropriate transfer function is selected according to the problem. Since there are 90 connections in our network architecture, there exist 4^{90} combinations of transfer functions, so that they can't be executed one by one. Among the four transfer functions we performed, we observed that the sigmoid function is optimal. The four transfer functions are as the following:

Sigmoid	$1/[1 + \exp(-x)]$
Gaussian	$\exp(-x^2)$
Hyperbolic tangent	$\tanh(x)$

Hyperbolic secant $\text{sech}(x)$

Training and Testing Neural Network

There are two main phases in the operation of a neural network: training and testing. In the training phase, 100 records of training data are used with 1000, 5000, 7500, 10000, 12500, 15000, 25000 iterations to let the neural network learn the relationship between input variables and output variables. In the testing phase, 25 records of testing data are used as input for the trained neural network. It was discovered from testing results that accuracy of prediction resulting from 10000 iterations is better than others. Iterations lower than 10000 tend to insufficient train the network, while iterations above 10000 show an over-learning tendency, that is, neural network will over-memorize the correlation between input and output variables and thus lose its flexibility in production analogies and deductions. For over 52% (13/25) of testing data, values of IRI predicted by neural network and actual values of IRI differ no more than 0.3. Only one record of the 25 records has a prediction value that differs from the actual value by more than 1, as shown in Table 3. We conclude that the appropriate iteration for this research is about 10000. The correlation coefficient and RMS (Root Mean Square) of 100 records of training data input are 0.84 and 0.068, respectively. The correlation coefficient increases as learning iteration increases, as shown in Figure 2. On the other hand, RMS decreases as learning iteration increases. When iteration count increases from 10000 to 25000, correlation coefficient still increases and RMS still decreases, but this phenomenon simply indicates that the neural network remembers competently the correlation between the input variables of 100 records of training data and its corresponding output variables. It loses its flexibility of analogy and deduction, so that the correlation coefficient from 25 unknown records of inputted testing data does not increase as the iteration number increases.

25 unique records of testing data were inputted into the neural network after it was trained with 100 records training data using 10000 iterations. The prediction result is shown in Table 4. The correlation coefficient between 25 testing records of input variable and its prediction values reaches 0.944, which is higher than that of training data, 0.84. This result indicates that this is a successful network architecture. 40% of the errors are no larger than 0.2, 72% of the errors are no larger than 0.5, and 96% no larger than 0.7.

Predicted IRI value via neural network learning and training approaches actual values, and its correlation coefficient reaches 0.944. Figure 3. illustrates that the accuracy of prediction does not centralize at any particular range. Whether for high, small or medium IRI value, the neural network has agreement in predictive accuracy.

Weight Effect of Each Distress Types

The effect of the 14 variables on the IRI is the main concern of our analysis. As shown in Figure 4, the greatest contribution is made by the input variable of the eighth node, “severe potholes”. In other words, a road section that has a worse IRI is usually accompanied by “severe potholes”. From another point of view, the IRI of a road section in which “severe potholes”—as measured by the manual visual evaluation process—occur frequently is always high. The decreasing order of percent contribution of input variables that succeed “severe potholes” is: left rutting (second node), digging road patching (sixth node), and right rutting (third node). There is occasional dispute over the issue of the correlation between rutting and pavement roughness. We observe from this research that it is clear that a road with considerable pavement roughness also has deep rutting. Deterioration of rutting is related to poor pavement materials, inappropriate construction, insufficient strength of the base layer, an excessive traffic burden as well as other factors. Severe rutting, to some extent, indicates the pavement’s poor quality; thus, it is closely related to pavement roughness. Among the 14 input variables, those that have only slight effects on pavement roughness are: alligator cracking, cracking, mild potholes, and bleeding. Pavement roughness is also affected by road level. Pavement roughness of provincial highways is less than that of county roads. As described above, any of the distress types and pavement roughness have a bi-directional causal relationship.

Even under the circumstances of it not being feasible to utilize rapid measurement equipment to perform pavement inspections, present manual visual inspection results may also be used as the input variables of the neural network we developed to obtain the determination of its corresponding IRI. The resulted IRI thus can be used as a kind of critical index of a pavement development management system. Besides, in Taiwan’s domestic pavement management, roughness measurement is generally applied to new road construction projects and is used as a measure for the acceptability of newly finished roads. Thus, it is clear that IRI can be

used to represent a pavement construction project's quality. Analysis results show that IRI can also be used to indicate pavement distresses or deterioration level.

Sensitivity Analysis of Pavement Distress Types

To learn the effect of partial repairs on pavement roughness, we use a back propagation neural network to analyze the variables' sensitivity. As shown above, the optimum result of our neural network model is obtained by training 10000 iterations. Thus, we perform the analysis of cracking, bleeding, potholes, stripping, corrugation, and man-holes by utilizing our neural network architecture with 10000 iterations.

Steps of the analysis process:

1. Sample selection:

50 records of distressed pavement data, which are not duplicates of the 100 records of training data, were randomly selected.

2. The samples were input into the neural network in order to proceed with the determination:

We used the neural network previously constructed and trained. The input variables and their order were the same as those described in the previous section, and the value of node at the output layer is the IRI. For example, the 50 records stated above are inspection data of 50 road sections with 27 road sections containing potholes. Thus the 14 variables of the 27 records were used as the input to the back-propagation neural network to predict the corresponding IRI.

3. A simulated prediction of non-distressed pavement was performed:

To simulate the IRI of non-potholed pavement or pavement after repair (assuming that the quality of repair reaches the non-potholed condition) under the same circumstances as the simulated environment of the 27 records mentioned above, we set the value of the pothole variable to 0, while the value of the other 13 input variables remained the same.

4. A correlation between repair surface area/number and Δ IRI was obtained:

To evaluate the effect of potholes number on IRI, we subtract the IRI value obtained in step 2 with the IRI value obtained in step 3. Next, we performed a regression analysis of the resulting difference value (Δ IRI) and number of repaired potholes to construct the correlation between the pothole repair number and Δ IRI.

5. Other distress types were analyzed:

For cracking, bleeding, stripping, corrugation, man-holes, we did the same as described in step 1 through step 4.

The analysis results, as shown in Figure 5, show that prediction results approach the corresponding actual value. We observe that predicted value of non-distress input is smaller than its original prediction value. Potholes, man-holes, and stripping have higher sensitivity in accordance to IRI, while cracking, bleeding, corrugation have less. The result shown in Figure 4 confirms this conclusion.

When rutting, cracking, bleeding, potholes, man-holes, stripping, corrugation, or any distress types occur, partial repair is a generally accepted solution. Yet, since repairs of different distress types of various surface areas have different effects on pavement, it is difficult for a maintenance management system to evaluate precisely the degree of improvement and the benefits of partial repair tasks. Simulation of these situations may solve this problem.

For example, assume there are ten locations with stripping within a 1-km road section (one stripping location is 20m; stripping less than 20m is also assumed as one stripping location). The 14 variables (the value of the one representing stripping is 10) of the road section are inputted into the neural network to proceed with prediction, then, a predicted IRI whose value approximates its actual measurement value is obtained. After that, the input variable that represents the stripping value is set to 0 to simulate the IRI value of non-stripping pavement, or repaired pavement that was originally stripped (assuming that the quality of reparation reaches the non-stripping condition). The regression models of reparation extent of the each distress type and IRI improvement values are shown in Figure 6. Except for corrugation, which shows an exponential regression model, the other regression models are linear. The non-increasing order of R^2 is caused by man-holes (0.95), cracking (0.93), and stripping (0.77). The R^2 values of bleeding, potholes, and corrugations are between 0.5 and 0.6, indicating that explanatory variance is insufficient and that some other causal factors need to be examined further. However, it is still statistically meaningful for us to evaluate the repair extent and the IRI improvement value.

CONCLUSIONS

In this research, artificial neural networks are employed in pavement roughness analysis. The three-layer back-propagation neural network proposed in this paper has strong prediction and analysis capability. Furthermore, the correlation coefficient of unknown samples examination is much higher than that of training samples, showing that it is a successful network architecture.

Pavement deterioration from time to time is characterized by distresses such as rutting, cracking, stripping, corrugation, potholes, man-holes, etc. The back propagation neural network is applied in this research to analyze the correlation between pavement distresses and IRI. The results of the analysis prove that IRI can be used either to evaluate the quality of pavement projects or to fully respond to the characteristics of the pavement deterioration process, which can be used as the basis for road maintenance ranking evaluation. In other words, rapid measurement of IRI using the Automatic Road Analyzer (ARAN) can simplify the works of traditional road-inspector visual inspection or miscellaneous manual rating works in the laboratory according to pavement images acquired by the image retrieval system. Based on the back-propagation neural network proposed in this paper, approximation of IRI may be obtained successfully by utilizing ratings obtained from pavement distress images and road level. Even though automatic IRI measuring devices are not common in Taiwan's basic road institutions, distress types and their extent or number within a 1-km road section obtained by present visual evaluation processes can also be used to determine IRI, and evaluation and planning may subsequently proceed based on it.

It was found that severe potholes, Digging/patching, and rutting have the highest correlation to IRI. Man-holes, stripping, and corrugation have less correlation. Cracking, alligator cracking, bleeding, and road level are the least related to IRI.

It was concluded that the sensitivity simulation analysis result based on the trained back-propagation neural network infers improvement in the IRI value of pavement after certain extent or amount of repair for each distress type.

REFERENCES

1. The Highway Development and Management Series, volumes two, The World Bank, part B2, pp.1-19, 2000.
2. Gulen, S., R. Wood, J. Weaver, and V. L. Anderson. Correlation of Present Serviceability Ratings with International Roughness Index, Transportation Research Record 1435, National Research Council, Washington, D.C., pp.27-37, 1994.
3. Janoff, M. S., J. B. Nick, and P. S. Davit Ketron. Pavement Roughness and Rideability, NCHRP Report 275, TRB, 1985.
4. ASTM E 867 “Standard Terminology Relation to Traveled Surface Characteristics”, Vol. 04.03 1996.
5. Haas, R., W. R. Hudson, and J. Zaniewski. Modern Pavement Management, Krieger Publishing Company, Florida, 1994.
6. The Highway Development and Management Series, volumes four, The World Bank, part c2, pp.52-56, 2000.
7. Eldin, N. N. and A. B. Senouci. A Pavement Condition-Rating Model Using Back-propagation Neural Network. *Microcomputers in Civil Engineering*, 10, 1995, pp.433-441.
8. Taha, Mahmoud A. and A. S. Hanna. Evolutionary Neural Network Model for the Selection of Pavement Maintenance Strategy. Transportation Research Board, 74th Annual Meeting, Preprint 95192, Washington, D.C., 1995.
9. Laurene Fauselt, *Fundamentals of Neural Networks Architectures, Algorithms, and Applications*, Florida Institute of Technology, 1994.

LIST OF TABLE TITLES

TABLE 1 Parameter Construction of Back-Propagation Neural Network

TABLE 2 Fourteen Categories of Neural Network Input Variables

TABLE 3 Testing Results of Various Training Iteration

TABLE 4 Actual Value and Prediction Value of 25 Records Testing Data

LIST OF FIGURE TITLES

FIGURE 1 Back-Propagation Neural Network Architecture

FIGURE 2 Correlation Between Correlation Coefficient and Training Iterations

FIGURE 3 Relationship between Target Value and Prediction Value

FIGURE 4 Weight of Input Variable

FIGURE 5 IRI Prediction Value of Non-Distress Condition (A Case of Potholes)

FIGURE 6 Correlation between Distress (Repair) Range and IRI Improvement

TABLE 1 Parameter Construction of Back-Propagation Neural Network

Parameter value	
Number of network layers	3
Number of nodes at input layer	14
Number of nodes at hidden layer	6
Number of nodes at hidden layer	1
Transfer function	Sigmoid
Number of connections	90
Training data	100
Testing data	25
Learning iteration	1000, 5000, 7500, 10000, 12500, 15000, 25000
Learning rate	0.01

TABLE 2 Fourteen Categories of Neural Network Input Variables

Node	Input Variable
1	The road level
2	left rutting
3	right rutting
4	alligator cracking
5	cracking
6	digging/patching
7	mild potholes
8	severe potholes
9	patching
10	bleeding
11	corrugation
12	stripping
13	mild man-holes
14	severe man-holes

TABLE 3 Testing Results of Various Training Iterations

Error \ Iteration Number	5000	10000	15000
Within 0.2	8/25	10/25	9/25
Within 0.3	13/25	13/25	13/25
Within 0.5	17/25	18/25	17/25
Within 0.7	23/25	23/25	19/25
Within 1	24/25	24/25	20/25

TABLE 4 Actual Value and Prediction Value of 25 Records Testing Data

Record	Actual value of IRI	Value of IRI predicted by neural network
1	2.97000	3.04177
2	2.78000	3.21953
3	2.76000	2.56387
4	3.34000	3.31494
5	3.15000	3.76363
6	4.07000	3.61808
7	2.86000	2.99967
8	5.18000	5.69365
9	4.87000	4.31010
10	3.07000	3.02100
11	5.69000	5.15410
12	3.92000	4.37860
13	7.28000	7.30150
14	4.08000	3.95959
15	3.44000	2.90473
16	2.76000	2.54302
17	3.58000	3.86048
18	4.15000	3.80594
19	6.40000	6.26429
20	4.91000	4.15301
21	2.34000	2.42122
22	3.12000	2.91801
23	6.34000	5.89703
24	5.68000	7.01909
25	4.76000	4.60546

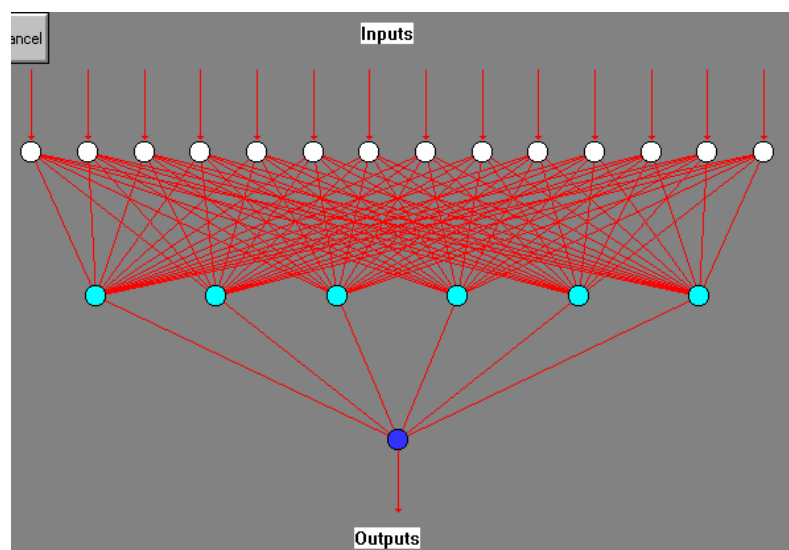


FIGURE 1 Back-Propagation Neural Network Architecture

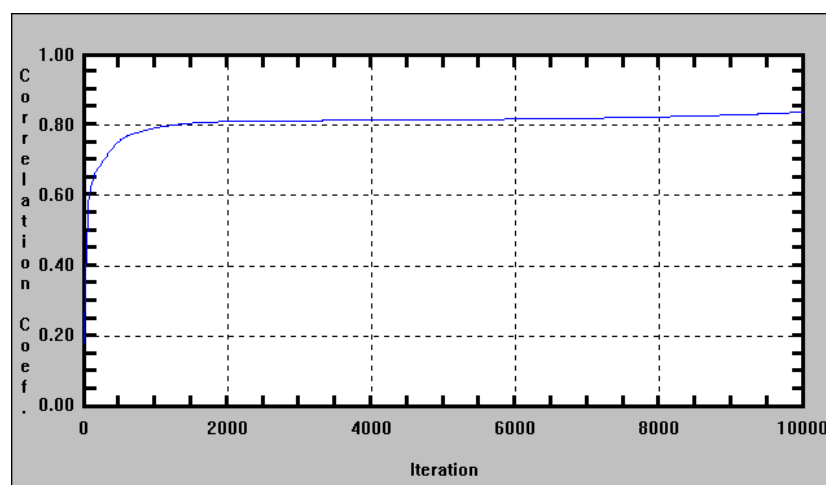


FIGURE 2 Correlation Between Correlation Coefficient and Training Iterations

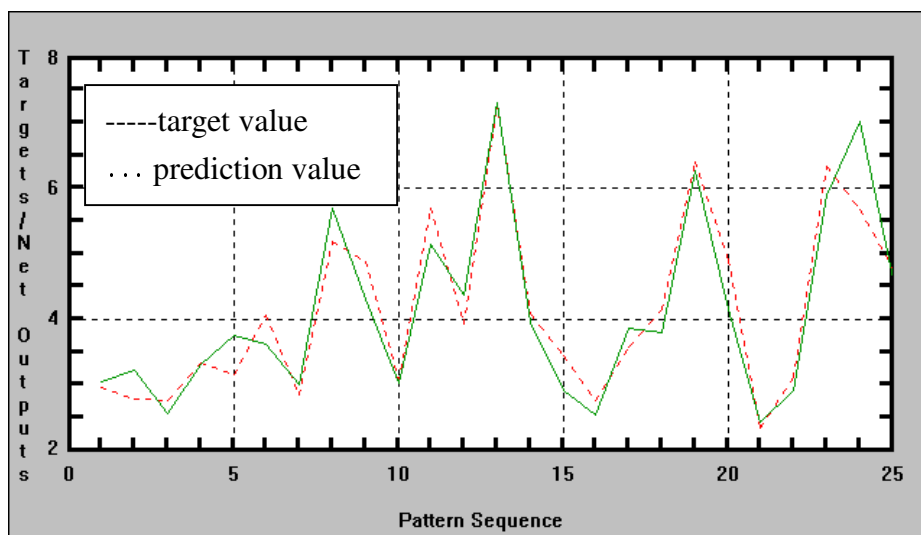


FIGURE 3 Relationship between Target Value (Actual Value of IRI) and Prediction Value (Value of IRI Predicted by Neural Network)

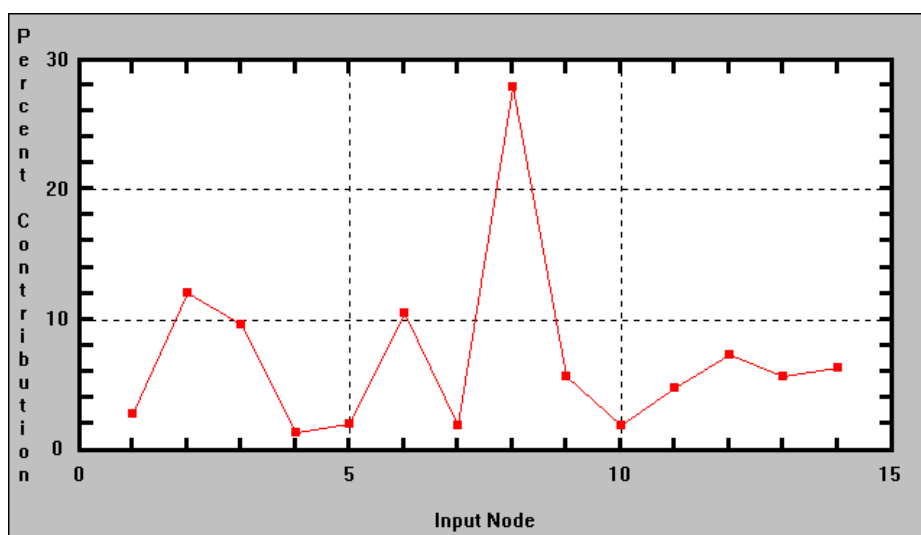


FIGURE 4 Weight of Input Variable

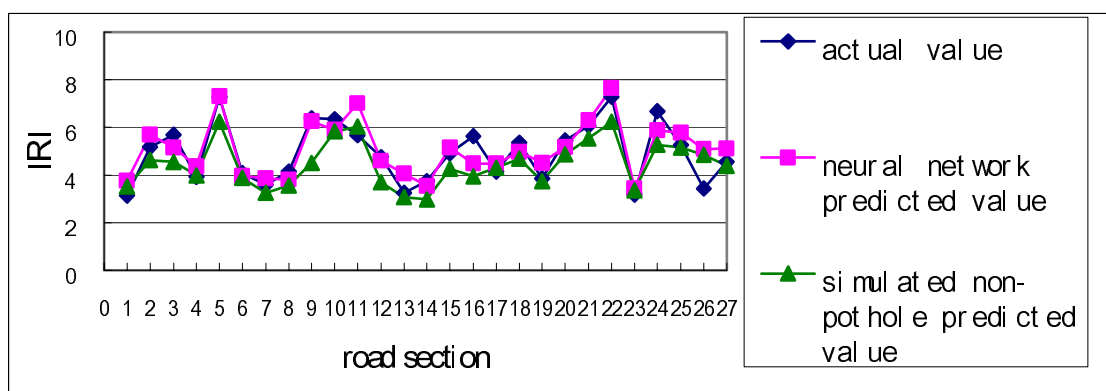
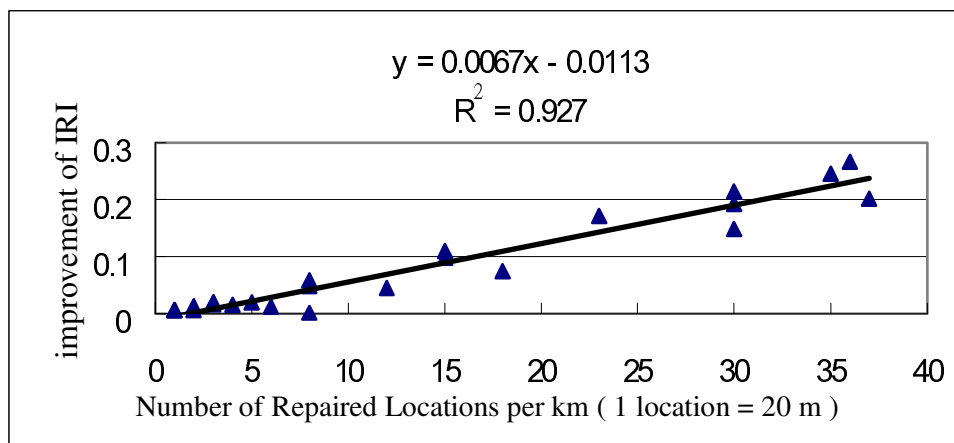
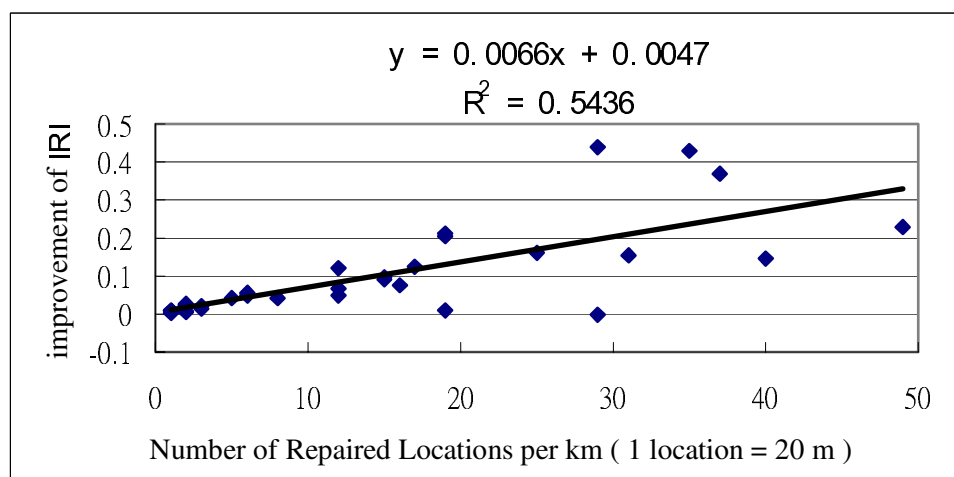


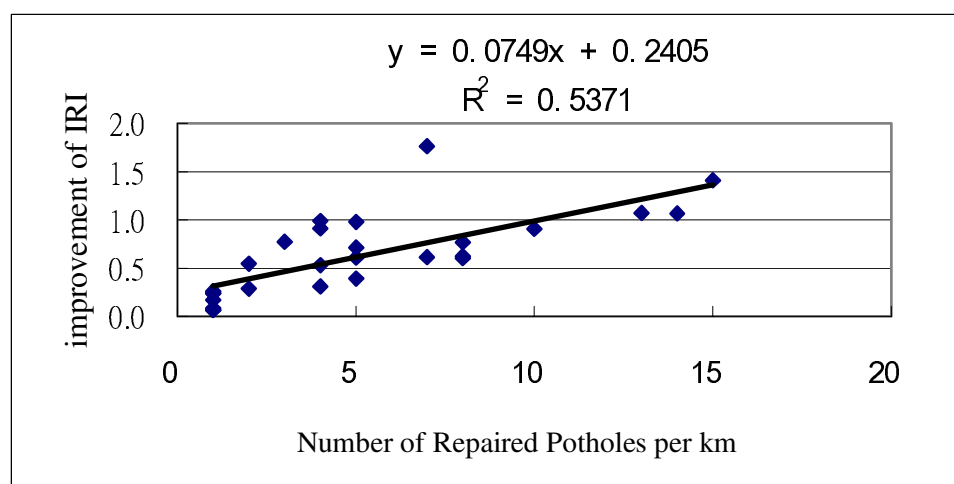
FIGURE 5 IRI Prediction Value of Non-Distress Condition (Pothole Case)



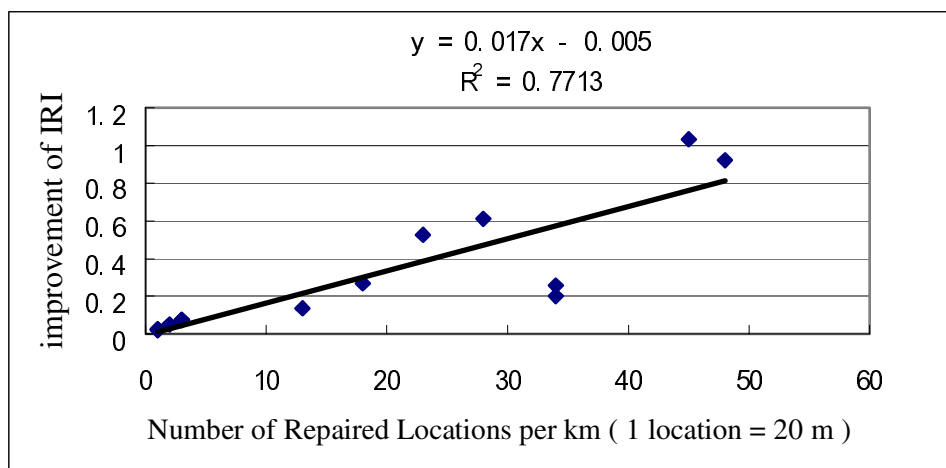
(a) Cracking Case



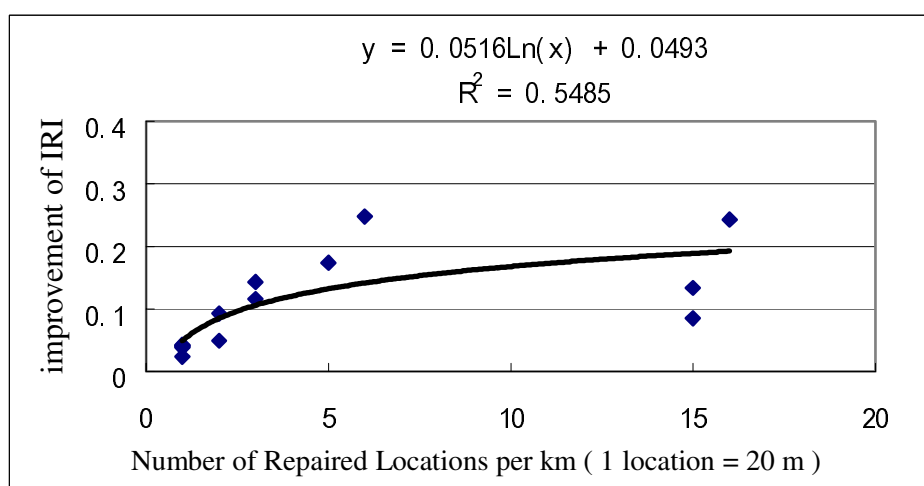
(b) Bleeding Case



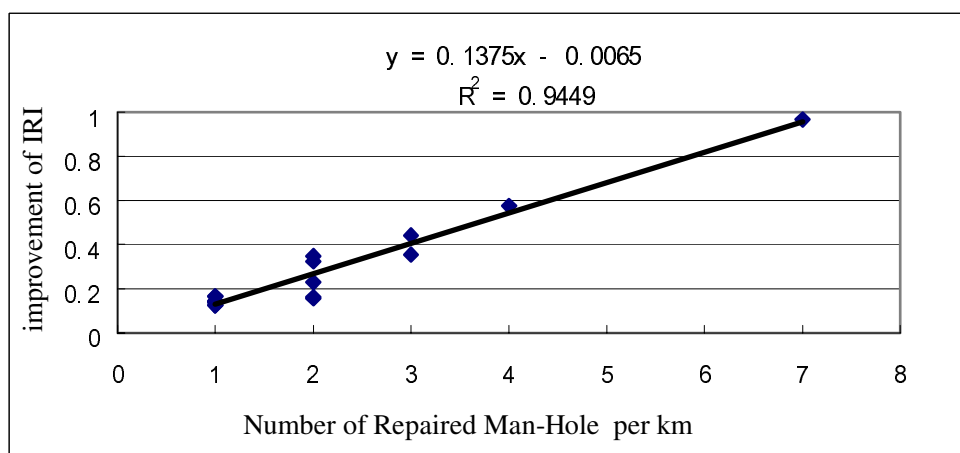
(c) Pothole Case



(d) Stripping Csse



(e) Corrugation Csse



(f) Man-Hole Csse

FIGURE 6 Correlation between Repair Extent and IRI Improvement